

Metal-insulator transition and superconductivity induced by Rh doping in the binary pnictides $RuPn$ ($Pn = P, As, Sb$)

Daigoro Hirai,^{1,*} Tomohiro Takayama,¹ Daisuke Hashizume,² and Hidenori Takagi^{1,2,3}

¹*Department of Advanced Materials, University of Tokyo and JST-TRIP, Kashiwa 277-8561, Japan*

²*RIKEN Advanced Science Institute, Wako 351-0198, Japan*

³*Department of Physics, University of Tokyo, Hongo 113-0033, Japan*

(Received 3 October 2011; revised manuscript received 17 March 2012; published 16 April 2012)

Binary ruthenium pnictides, RuP and RuAs, with an orthorhombic MnP structure, were found to show a metal to a nonmagnetic insulator transition at $T_{MI} = 270$ and 200 K, respectively. In the metallic region above T_{MI} , a structural phase transition, accompanied with a weak anomaly in the resistivity and the magnetic susceptibility, indicative of a pseudogap formation, was identified at $T_s = 330$ and 280 K, respectively. These two transitions were suppressed by substituting Ru with Rh. We found superconductivity with a maximum $T_c = 3.7$ and 1.8 K in a narrow composition range around the critical point for the pseudogap phase, Rh content $x_c = 0.45$ and 0.25 for $Ru_{1-x}Rh_xP$ and $Ru_{1-x}Rh_xAs$, respectively, which may provide us with a nonmagnetic route to superconductivity at a quantum critical point.

DOI: [10.1103/PhysRevB.85.140509](https://doi.org/10.1103/PhysRevB.85.140509)

PACS number(s): 74.70.Xa, 71.30.+h, 74.25.Dw, 74.40.Kb

The relationship between superconductivity and other collective electronic states has been a long-standing enigma in condensed-matter physics. In a variety of systems with distinct chemical characters, including cuprates,¹ heavy fermions,² organics,³ and, more recently, iron pnictide,⁴ superconductivity was found in a narrow region near the critical border to magnetism as a function of pressure and doping. Superconductivity has also been observed at a critical border to classes of electronic orderings other than magnetic ordering, including charge ordering⁵⁻⁷ and charge density wave,^{8,9} although T_c remains relatively low.

Stimulated by the discovery of iron pnictide superconductors, we have been exploring possible superconductivity in Ru pnictides. $4d$ Ru has the same d -electron number as $3d$ Fe and is in general less magnetic. A series of binary compounds $RuPn$ ($Pn = P, As, \text{ and } Sb$) has been reported to crystallize in a MnP-type orthorhombic structure (space group $Pnma$).¹⁰⁻¹² In this crystal structure (see the inset to Fig. 1), $RuPn_6$ octahedra form a face-sharing chain along the a axis. The chains are connected by the edges and Ru forms a distorted triangular lattice within the bc plane.

We discovered two sequential phase transitions in RuP and RuAs: a weak transition from a metal to a pseudogap phase accompanied with the superstructure formation at high temperature ($T_s = 330$ K for RuP and 280 K for RuAs) and a first-order transition to a nonmagnetic insulator at low temperature ($T_{MI} = 270$ K for RuP and 200 K for RuAs). We suppressed those two transitions by Rh doping for Ru and found superconductivity at the critical point for the “pseudogap phase.” Although the microscopic origin of the transitions remains yet to be clarified, the discovery should provide a playground for superconductivity at a nonmagnetic critical point. Herein, we present the transport, magnetic, thermal, and structural properties of $Ru_{1-x}Rh_xP$ and $Ru_{1-x}Rh_xAs$, with emphasis on the discovery of two phase transitions and superconductivity at a critical point, and discuss the possible origin of the phase transitions.

Polycrystalline samples of $RuPn$ ($Pn = P, As, \text{ and } Sb$) and Rh-doped samples $Ru_{1-x}Rh_xP$ and $Ru_{1-x}Rh_xAs$ were

prepared by a conventional solid-state reaction. A mixture of Ru metal, Rh metal, and pnictogen elements was sintered in an evacuated quartz tube initially at 550 °C for 10 h and then at 1050 °C for $Ru_{1-x}Rh_xP$, 950 °C for $Ru_{1-x}Rh_xAs$, and 900 °C for RuSb for 48 h. An excess of pnictogen elements was added to compensate for the loss due to volatilization. The sintered pellet was reground, repelletized, and sintered again for 72 h. The x-ray diffraction (XRD) pattern of the obtained sample [Fig. 2(a)] indicated the formation of a single phase within the given resolution, except for heavily Rh-doped RuP containing a trace amount of elemental Rh of the order of 1%. Magnetic, transport, and thermal measurements were conducted by a superconducting quantum interference device (SQUID) magnetometer and a Physical Property Measurement System (PPMS: Quantum Design). Electrical resistivity $\rho(T)$ above 350 K was measured separately by a four-probe method in a furnace with flowing N_2 gas. Very small single crystals of RuP, less than 100 μm in size, were grown out of Sn flux and used for the structural analysis.

All of the three pnictides, RuP, RuAs, and RuSb, were found to be metallic at room temperature with a magnitude of resistivity ~ 1 m Ω cm. On cooling, a metal-insulator transition was clearly observed for RuP and RuAs at $T_{MI} = 270$ and 200 K, shown in Fig. 2(b) and, below the T_{MI} , $\rho(T)$ shows an insulating behavior. The presence of tiny but clear hysteresis around the T_{MI} indicates that the metal-insulator transitions are of first order. In the case of RuAs, we observe a much broader transition than in RuP, which we believe represents the presence of some inhomogeneity in the RuAs sample. RuSb was found to be metallic down to the lowest temperature measured.

The magnetic susceptibility $\chi(T)$ [Fig. 2(b)] in the metallic phase above T_{MI} is less than 10^{-4} emu/mol, which may be ascribed to the Pauli paramagnetic susceptibility of a metal with a moderate density of states (DOS). At T_{MI} for RuP and RuAs, $\chi(T)$ shows an almost discontinuous drop to a negative value with hysteresis, which is comparable to the expected core diamagnetism.¹³ This suggests that the low-temperature insulating state is nonmagnetic. A recent

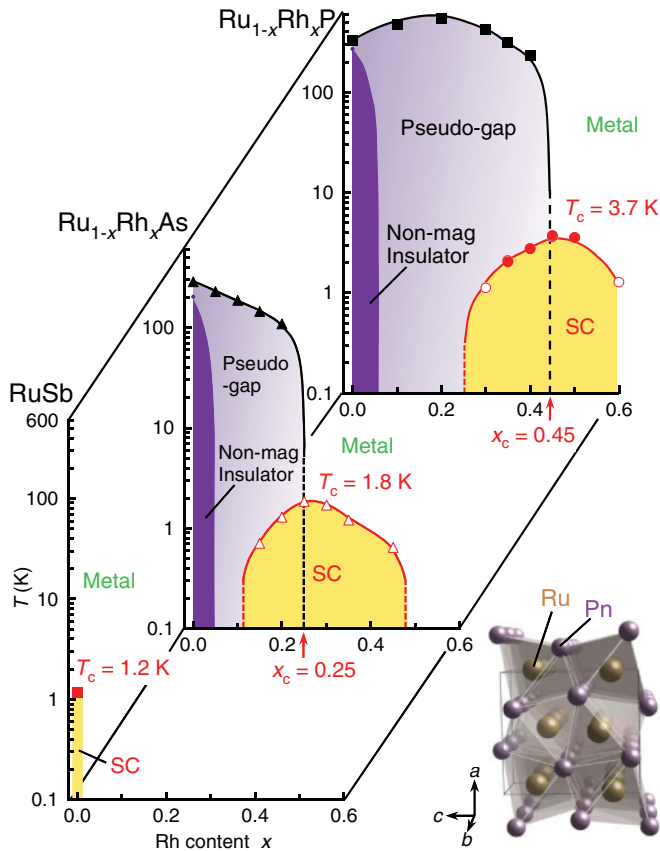


FIG. 1. (Color online) Electronic phase diagrams of $\text{Ru}_{1-x}\text{Rh}_x\text{P}$, $\text{Ru}_{1-x}\text{Rh}_x\text{As}$, and RuSb as functions of Rh doping. Solid squares and triangles in $\text{Ru}_{1-x}\text{Rh}_x\text{P}$ and $\text{Ru}_{1-x}\text{Rh}_x\text{As}$ correspond to the transition temperatures to the pseudogap phase T_s determined from the minima in $\rho(T)$ curves. Solid and open circles in $\text{Ru}_{1-x}\text{Rh}_x\text{P}$ represent the superconducting transition temperatures T_c determined from the magnetization and the specific-heat measurements, respectively. Open triangles in $\text{Ru}_{1-x}\text{Rh}_x\text{As}$ indicate T_c determined from the heat capacity data. The inset shows the crystal structure of RuPn ($Pn = \text{P, As, and Sb}$).

muon spin relaxation (μSR) experiment on RuAs (Ref. 14) also supports the presence of a nonmagnetic ground state. The systematic suppression of a metal-insulator transition on going from P, As, to Sb would reflect the increased bandwidth due to the enhanced p - d hybridization. The increase of Pauli paramagnetic susceptibility from P, As, to Sb, however, suggests the increased density of states, which contradicts the increased bandwidth and therefore requires invoking additional ingredients.

Closely inspecting the poorly metallic state of RuP and RuAs above T_{MI} , we notice an additional anomaly at $T_s = 330$ and 280 K, respectively. As shown in the inset to Fig. 2(b), at T_s , there is a minimum in $\rho(T)$ and a maximum in $\chi(T)$. It appears that the anomaly at T_s represents a precursor to the metal to nonmagnetic insulator transition in that $\rho(T)$ increases and $\chi(T)$ decreases below T_s .

From $\rho(T)$ and $\chi(T)$ data alone, it is not clear whether or not T_s represents a well-defined phase transition. However, the single-crystal x-ray structural analysis on a RuP shown in Fig. 2(c) indicates clearly that it is a phase transition. The

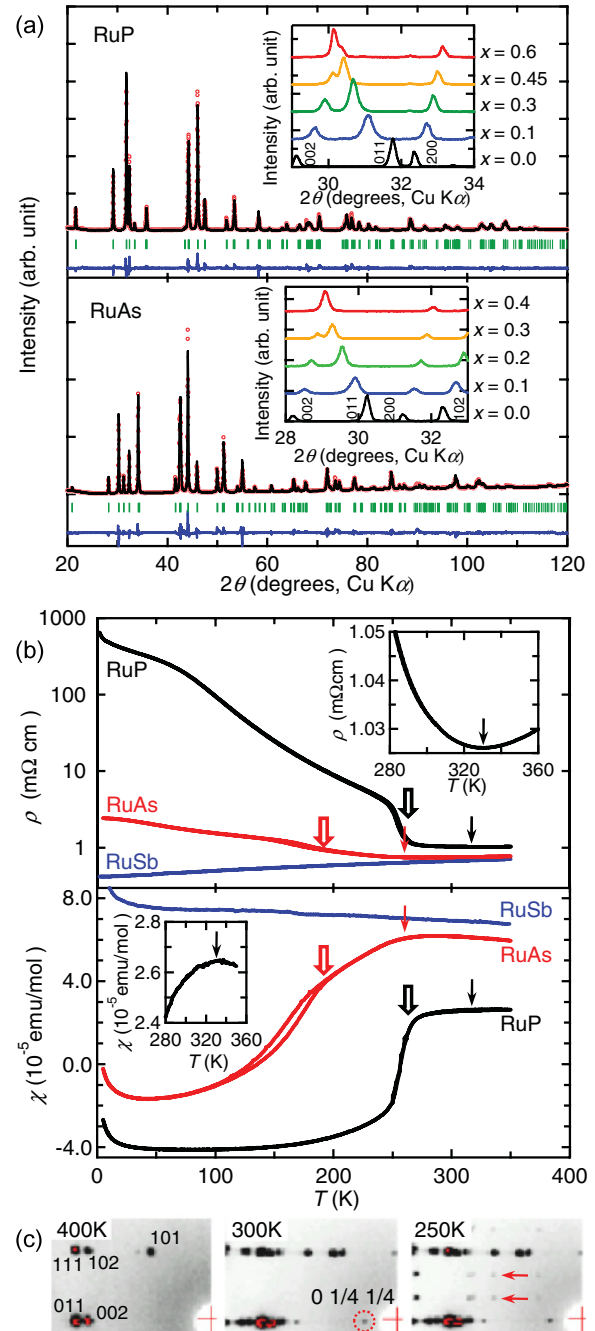


FIG. 2. (Color online) (a) XRD patterns of (upper panel) RuP and (lower panel) RuAs . The open circles, solid line, and lower solid line represent observed, calculated, and difference XRD patterns, respectively. Tick marks indicate the position of allowed reflections. The insets show an enlarged area of the XRD pattern, showing a systematic change with Rh concentration for $\text{Ru}_{1-x}\text{Rh}_x\text{P}$ and $\text{Ru}_{1-x}\text{Rh}_x\text{As}$. (b) Temperature dependence of (upper panel) resistivity $\rho(T)$ in zero applied field and (lower panel) dc magnetic susceptibility $\chi(T)$ under an applied field of 1 T for RuP , RuAs , and RuSb . Open and solid arrows indicate the metal to nonmagnetic insulator transitions and high-temperature structural transitions in RuP and RuAs , respectively. The insets show the $\rho(T)$ and $\chi(T)$ anomaly associated with the phase transition at $T_s = 330$ K in RuP . (c) Single-crystal x-ray diffraction patterns for RuP measured at 400, 300, and 250 K. The reflections at 400 K are indexed based on the orthorhombic cell.

crystal structure of RuP at 400 K (above T_s) was refined well with an orthorhombic $Pnma$ space group, as reported in Ref. 10. On cooling, superlattice spots $h k/4 l/4$ appear just below $T_s = 330$ K, indicating the fourfold structural modulation within the bc plane along the [011] direction. By lowering the temperature further, additional spots indicative of tripling of the a axis, the chain direction, emerge at $T_{MI} = 270$ K. The crystal structures below T_s and below T_{MI} remain yet to be refined. In the RuAs polycrystalline powder, we observed the superlattice peaks in the powder pattern at T_s and T_{MI} , analogous to those observed for the RuP single crystal.

Considering the three-dimensional crystal structure of RuP, a nesting-driven charge density wave (CDW) in its simplest form is highly unlikely to describe the insulating ground state with the whole Fermi surface gapped. A band-structure calculation indeed indicated the presence of complicated and multiple Fermi surfaces and a nesting-driven CDW is highly improbable to occur. A more elaborate picture, such as local spin dimer formation associated with orbital ordering, should be invoked to account for the nonmagnetic insulating state. A metal to nonmagnetic insulator transition in three-dimensional complex transition-metal oxides has been observed, for example, in Magnéli phase vanadium and titanium oxides,¹⁵ $Tl_2Ru_2O_7$,¹⁶ $CuIr_2S_4$,¹⁷ $MgTi_2O_4$,¹⁸ and $LiRh_2O_4$.¹⁹ In all these compounds, orbital ordering is believed to play a key role in realizing the nonmagnetic, spin singlet ground state. Interestingly, in $LiRh_2O_4$, the orbital ordering, with weak $\rho(T)$ and $\chi(T)$ anomalies similar to those observed in Ru pnictides, occurs at a higher temperature than the first-order metal-insulator transition and gives rise to a reduced dimensionality of the itinerant electrons, which acts as a precursor to the metal-nonmagnetic insulator transition.¹⁹

Inspired by the close link between electronic order and superconductivity recognized in a variety of systems, we have attempted to suppress the two transitions in RuP and RuAs by doping. We found that Rh doping for Ru systematically suppresses the two transitions. As seen from $\rho(T)$ and $\chi(T)$ shown in Fig. 3, upon Rh doping, the first-order transition at T_{MI} is rapidly suppressed and is absent already at 10% doping level for both RuP and RuAs. The transition at T_s appears to be much more robust against doping than the metal-insulator transition. Even with more than 10% doping, we see a broad peak in $\chi(T)$ and a minimum in $\rho(T)$ representing T_s . Below T_s , an anomalous and poorly metallic state is realized. First of all, $\rho(T)$ shows a very weak increase on cooling but appears to approach a finite value. $\chi(T)$ shows a pronounced decrease on cooling sometimes even to a diamagnetic regime, suggesting reducing DOS. The reduction of magnetic susceptibility is analogous to those observed, for example, in the underdoped cuprates,²⁰ and indicative of the presence of a pseudogap. In this Rapid Communication, we call this poorly metallic phase below T_s as a “pseudogap” phase. This is again suggestive of the transition at T_s being a precursor to the nonmagnetic insulator phase observed in the undoped compounds.

Eventually the pseudogap transition disappears at $x_c = 0.45$ for RuP and at $x_c = 0.25$ for RuAs, as clearly seen in Fig. 3. In support of the presence of a well-defined critical point, the very clear anomaly in the doping dependence of Debye temperature Θ_D and the electronic specific-heat coefficient γ was observed

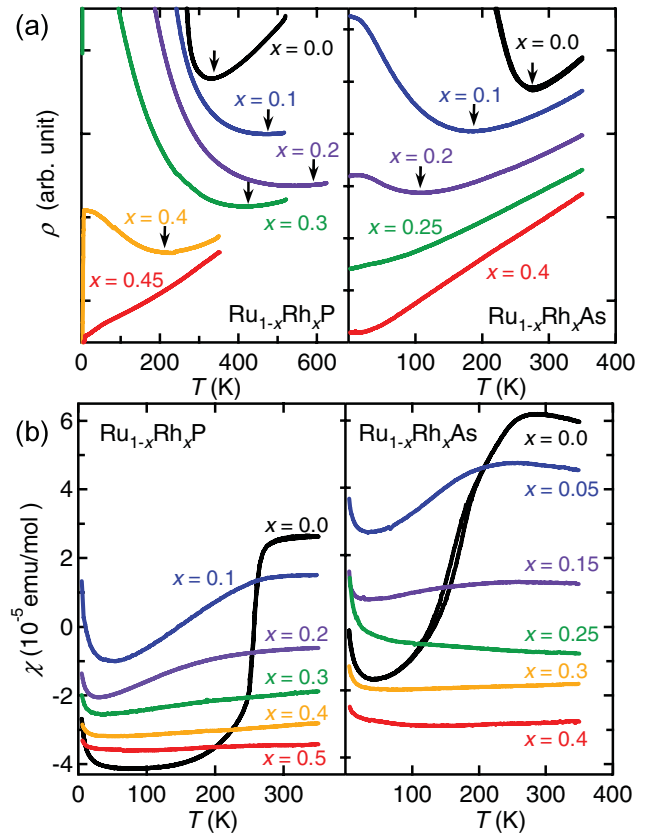


FIG. 3. (Color online) Temperature-dependent (a) resistivity ($\rho(T)$) and (b) magnetic susceptibility ($\chi(T)$) for $Ru_{1-x}Rh_xPn$ ($Pn = P$ and As). dc magnetic susceptibility was measured under an applied magnetic field of 1 T. The arrows in (a) indicate the minima of the $\rho(T)$ curve, defined as the pseudogap transition temperature T_s .

at x_c , indicative of the presence of a phase transition involving both electrons and lattices.

We discovered superconductivity at the critical point for the pseudogap phase. As shown in Fig. 4(a), zero resistance and full diamagnetic shielding, indicative of a superconducting transition, are observed below $T_c = 3.7$ and 1.8 K for the samples with the critical Rh content x_c , $Ru_{0.55}Rh_{0.45}P$ and $Ru_{0.75}Rh_{0.25}As$, respectively. The electronic specific heat $C_e(T)$ of those two samples were estimated by subtracting the normal-state $C_N(T)$ under 9-T magnetic field, which is well above the upper critical field $\mu_0 H_{c2}(0)$, and adding the γT term with γ obtained from the extrapolation of $C_N(T)/T$ to $T = 0$. The electronic specific-heat coefficient γ was estimated as 1.3 mJ/mol K² for $Ru_{0.55}Rh_{0.45}P$ and 3.0 mJ/mol K² for $Ru_{0.75}Rh_{0.25}As$, which is quite moderate for a $4d$ intermetallic compound. $C_e(T)$ shows a large jump at T_c both for $Ru_{0.55}Rh_{0.45}P$ and $Ru_{0.75}Rh_{0.25}As$, evidencing the bulk superconductivity. The rapid decrease of $C_e(T)/T$ below T_c in $Ru_{0.55}Rh_{0.45}P$ suggests fully gapped superconductivity, which is very likely an s wave. The slow decrease of $C_e(T)/T$ in $Ru_{0.75}Rh_{0.25}As$ at a glance appears to imply a gapless superconductivity, but considering the pronounced inhomogeneity in the RuAs system, we suspect that it reflects a distribution of an inhomogeneous gap rather than gap node(s).

As seen from the specific-heat data $C(T)$ and magnetization data $\chi(T)$ for the samples with different doping

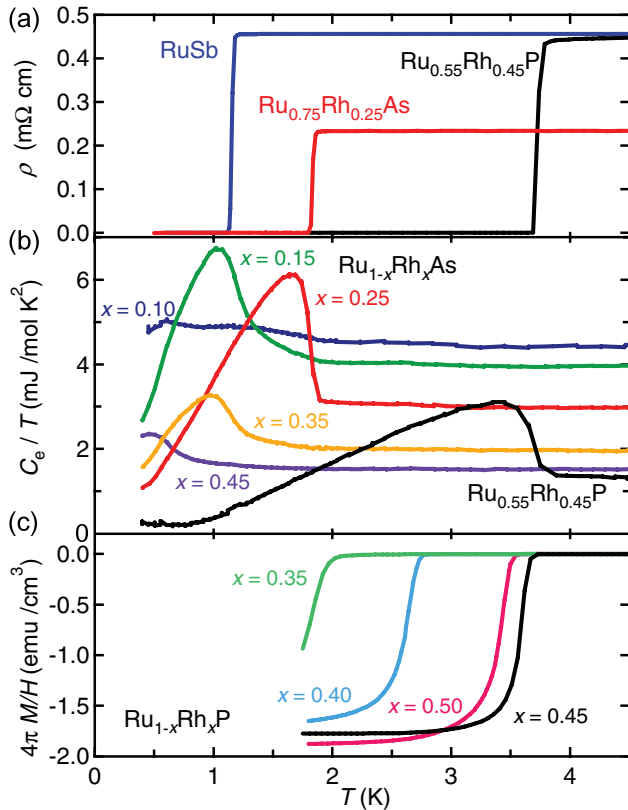


FIG. 4. (Color online) Superconducting transitions observed in Ru pnictides. (a) Temperature-dependent resistivity $\rho(T)$ of $\text{Ru}_{0.55}\text{Rh}_{0.45}\text{P}$, $\text{Ru}_{0.75}\text{Rh}_{0.25}\text{As}$, and RuSb . (b) Electronic specific heat divided by temperature C_e/T for $\text{Ru}_{0.55}\text{Rh}_{0.45}\text{P}$ and $\text{Ru}_{1-x}\text{Rh}_x\text{As}$ ($x = 0.1, 0.15, 0.25, 0.35, \text{ and } 0.45$). (c) dc magnetization data at low temperatures under applied magnetic field of 20 Oe for $\text{Ru}_{1-x}\text{Rh}_x\text{P}$ ($x = 0.35, 0.40, 0.45, \text{ and } 0.50$).

levels shown in Figs. 4(b) and 4(c), superconductivity was observed in a limited region around the critical point x_c and transition temperature T_c peaked at x_c both for $\text{Ru}_{1-x}\text{Rh}_x\text{P}$ and $\text{Ru}_{1-x}\text{Rh}_x\text{As}$. The interplay between the criticality and superconductivity in doped RuP and RuAs can be illustrated visually as a phase diagram shown in Fig. 1. The rapid collapse of the nonmagnetic insulating phase upon doping may suggest that the accommodation of an integer number of electrons is an important ingredient for the emergence of a

nonmagnetic insulator phase below T_{MI} . On the other hand, the insensitivity of T_s and systematic suppression of the pseudogap behavior upon doping might mean a local character of the phase transition. The presence of a superconducting dome centered at the critical point clearly indicates the link between the criticality to the ordering below T_s and superconductivity.

Comparing $\text{Ru}_{1-x}\text{Rh}_x\text{P}$ and $\text{Ru}_{1-x}\text{Rh}_x\text{As}$, it is clear that the T_s ordering is suppressed more readily for $\text{Ru}_{1-x}\text{Rh}_x\text{As}$ in which T_s for the undoped compound and x_c are much lower for RuAs than RuP. Possibly reflecting this, the “optimum” T_c is higher for $\text{Ru}_{1-x}\text{Rh}_x\text{P}$ ($T_c = 3.7$ K) than $\text{Ru}_{1-x}\text{Rh}_x\text{As}$ ($T_c = 1.8$ K). It might be interesting to infer here that $\text{Ru}_{0.55}\text{Rh}_{0.45}\text{P}$ has a smaller electronic specific-heat coefficient ($\gamma \sim 1.3$ mJ/mol K²) than that of $\text{Ru}_{0.75}\text{Rh}_{0.25}\text{As}$ ($\gamma \sim 3.0$ mJ/mol K²). We argue that such an anticorrelation between DOS and T_c , opposite to what is predicted from BCS theory, might imply the vital role of the energy scale of criticality. The T_s ordering appears to be suppressed completely for RuSb, but superconductivity with a lower T_c than $\text{Ru}_{1-x}\text{Rh}_x\text{P}$ and $\text{Ru}_{1-x}\text{Rh}_x\text{As}$, $T_c = 1.2$ K, was still observed, as seen in Fig. 4(a). This might suggest that RuSb is located not far away from the hidden critical point.

In conclusion, we found two sequential transitions in binary pnictides RuP and RuAs: a high-temperature transition to a pseudogap phase at T_s and a low-temperature metal to nonmagnetic insulator at T_{MI} . To clarify the physics behind those two transitions, the refinement of the lattice distortion pattern below T_s and T_{MI} should have a high priority. Rh doping was found to suppress those two transitions. In a narrow doping region around a critical point for the pseudogap phase, superconductivity was discovered with maximum T_c of 3.7 K for $\text{Ru}_{0.55}\text{Rh}_{0.45}\text{P}$ and 1.8 K for $\text{Ru}_{0.75}\text{Rh}_{0.25}\text{As}$, giving rise to a playground for the superconductivity at a critical point. We emphasize here that the critical point here is neither antiferromagnetic nor ferromagnetic, as is usually the case in widely discussed superconductivity at a critical point.

We thank A. Mackenzie, P. Radaelli, T. Mizokawa, Y. Katsura, D. Nishio-Hamane, and A. Yamamoto for stimulating discussions. This work was partly supported by a Grant-in-Aid for Scientific Research (S) (Grant No. 19104008) and a Grant-in-Aid for Scientific Research on Priority Areas (Grant No. 19052008).

*Present address: Department of Chemistry, Princeton University, Princeton, New Jersey 08540, USA.

¹S. Huffner, M. A. Hossain, A. Damaceli, and G. A. Sawatzky, *Rep. Prog. Phys.* **71**, 062501 (2008).

²N. D. Mathur, F. M. Groshe, S. R. Julian, I. R. Walker, D. M. Freye, R. K. W. Haselwimmer, and G. G. Lonzarich, *Nature (London)* **394**, 39 (1998).

³T. Lorenz, M. Hofmann, M. Grüninger, A. Freimuth, G. S. Uhrig, M. Dumm, and M. Dressel, *Nature (London)* **418**, 614 (2002).

⁴Y. Kamihara, T. Watanabe, M. Hirano, and H. Hosono, *J. Am. Chem. Soc.* **130**, 3296 (2008).

⁵T. Yamauchi, Y. Ueda, and N. Mori, *Phys. Rev. Lett.* **89**, 057002 (2002).

⁶M. Ito, H. Kurisaki, F. Nakamura, T. Fujita, T. Suzuki, J. Hori, H. Okada, and H. Fujii, *J. Appl. Phys.* **97**, 10B112 (2005).

⁷H. Suzuki, T. Furubayashi, G. Cao, H. Kitazawa, A. Kamimura, K. Hirata, and T. Matsumoto, *J. Phys. Soc. Jpn.* **68**, 2495 (1999).

⁸E. Morosan, H. W. Zandbergen, B. S. Dennis, J. W. G. Bos, Y. Onose, T. Klimczuk, A. P. Ramirez, N. P. Ong, and R. J. Cava, *Nat. Phys.* **2**, 544 (2006).

⁹A. F. Kusmartseva, B. Sipos, H. Berger, L. Forro, and E. Tutis, *Phys. Rev. Lett.* **103**, 236401 (2009).

¹⁰S. Rundqvist, *Acta Chem. Scand.* **16**, 287 (1962).

¹¹R. D. Heyding and L. D. Calvert, *Can. J. Chem.* **39**, 955 (1961).

- ¹²K. Endresen, S. Furuseth, K. Selte, A. Kjekshus, T. Rakke, and A. F. Andresen, *Acta Chem. Scand. A* **31**, 249 (1977).
- ¹³P. W. Selwood, *Magnetochemistry* (Interscience, New York, 1956), 2nd ed., p. 78.
- ¹⁴Y. Ishii (private communication).
- ¹⁵M. Marezio, D. B. McWhan, P. D. Dernier, and J. P. Remeika, *Phys. Rev. Lett.* **28**, 1390 (1972).
- ¹⁶S. Lee, J.-G. Park, D. T. Adroja, D. Khomskii, S. Streltsov, K. A. Mcewen, H. Sakai, K. Yoshimura, V. I. Anisimov, D. Mori, R. Kanno, and R. Ibberson, *Nat. Mater.* **5**, 471 (2006).
- ¹⁷P. G. Radaelli, Y. Horibe, M. J. Gutmann, H. Ishibashi, C. H. Chen, R. M. Ibberson, Y. Koyama, Y.-S. Hor, V. Kiryukhin, and S.-W. Cheong, *Nature (London)* **416**, 155 (2002).
- ¹⁸M. Schmidt, W. Ratcliff, P. G. Radaelli, K. Refson, N. M. Harrison, and S. W. Cheong, *Phys. Rev. Lett.* **92**, 056402 (2004).
- ¹⁹Y. Okamoto, S. Niitaka, M. Uchida, T. Waki, M. Takigawa, Y. Nakatsu, A. Sekiyama, S. Suga, R. Arita, and H. Takagi, *Phys. Rev. Lett.* **101**, 086404 (2008).
- ²⁰T. Watanabe, T. Fujii, and A. Matsuda, *Phys. Rev. Lett.* **84**, 5848 (2000).